Laser Induced Micromachining and Preliminary Experiments on Manufacturing of Micro-channel on Mild Steel

Sanasam Sunderlal Singh, S.N. Joshi and Alika Khare

Abstract Laser-Induced Micromachining (LIMM) is a non-conventional machining process in which a high power laser beam is focused over the work surface in order to remove the material selectively. The material is removed through melting, evaporation and plasma formation. LIMM offers better machining efficiency than other non-conventional machining processes in terms of the machining rate, efficient debris removal, better surface morphology and capability to machine wide range of materials irrespective of its hardness and electrical conductivity. Further precision can be obtained by confining the laser induced plasma plume from the surface using an external magnetic field or electric field. This chapter deals with a brief introduction and basic principle of laser induced micromachining. This is followed by a discussion on various configurations of LIMM. Further, a review on numerical and experimental studies of the laser induced micromachining is presented. At the end of the chapter, preliminary experimental work on laser induced micromachining of mild steel has been reported.

Keywords Laser induced micromachining · Micro channel · Numerical modeling of LIMM

1 Introduction

To fulfill the need and requirement of modern society in terms of MEMS devices, the demand for miniaturized features like fuel injection nozzles in automobiles, micro holes in electrical printed circuit board and textile industries, nano level

S.S. Singh · S.N. Joshi (✉)
Department of Mechanical Engineering, Indian Institute of Technology Guwahati, Guwahati 781039, Assam, India
e-mail: snj@iitg.ernet.in

A. Khare
Department of Physics, Indian Institute of Technology Guwahati, Guwahati 781039, Assam, India

S.N. Joshi and U.S. Dixit (eds.), *Lasers Based Manufacturing*,
Topics in Mining, Metallurgy and Materials Engineering,
DOI 10.1007/978-81-322-2352-8_11

surface finish on complex geometry, micro fluidic channels have been tremendously increasing. This has lead to the development of micromachining such as laser micromachining, ultrasonic micromachining, micro electrical discharge machining, electrochemical micromachining, etc. Micromachining indicates machining in the range of 1–999 μm. In recent years, laser beam micromachining (LIMM) has emerged as one of the dominant non-contact processing tools in the fabrication of micro-components. LIMM can remove material in very small amount (in micron range), while traditional machining removes material in macro scale. Application of lasers have advantages such as narrow cut, minimum heat affected zone (HAZ), better accuracy, smooth and flat edges, minimal deformation of the workpiece and fast cutting of intricate profile cut and fast adaptation to changes in manufacturing programs.

1.1 Laser Induced Micromachining

Laser, an acronym of light amplification by stimulated emission of radiation, is a device that emits light through the process of stimulated emission. It comprises of three main components namely the lasing medium (active medium), pump (means of exciting the lasing medium into its appropriate higher energy states) and optical feedback system or optical cavity comprising of two mirrors as shown in Fig. 1 (Silfvest 2004). One of the mirrors is made partially reflecting making the laser beam to come out of the cavity for useful purpose.

One can classify laser based on the lasing medium: Gas laser, Liquid laser, Solid state laser, Semiconductor, Free electron laser etc. Laser can be operated either in continuous wave (CW) mode or in pulsed mode. The main properties of laser are: high brightness, monochromatic, low divergence and high spatial and temporal coherence.

Laser Induced Micromachining (LIMM) can be applied to any material while traditional machining processes have to choose compatible tools for materials with different strength or hardness. It is difficult to machine hard material or brittle material such as ceramics by traditional machining processes. However, laser

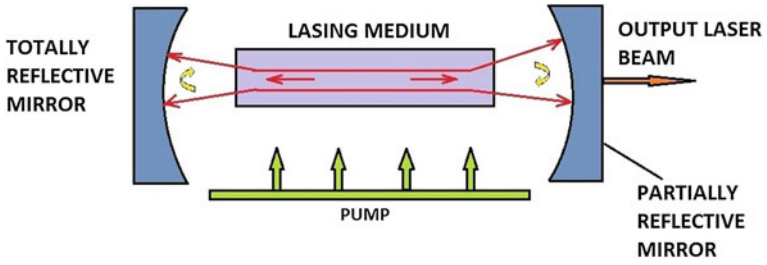

Fig. 1 Schematic diagram of laser system

machining can easily machine such materials with high precision. In LIMM, laser beam is focused by a lens on the work surface, removing a small portion of the material by melting and vaporization. The process of removing the material is known as ablation. It is generally accepted that two phenomena happen during the ablation process i.e. photochemical ablation and photo-thermal ablation. Photo-chemical ablation involves the absorption of photons leading directly to bond breaking in the material without any intermediate heat dissipation. It uses UV photons having energies 3–7 eV (Johan 2004), which is used to break the chemical bonds directly. Alternatively, multi-photon process can be utilized with the longer wavelength laser. This phenomenon is generally used for machining of polymers. In photo-thermal ablation, deposited energy is converted into heat and decomposes the material surface in the focal volume. The processes involved are: heating, melting, ablation of the surfaces etc. The focal intensity of laser influences the vaporization rate and high vaporization rate causes a shockwave that can reach pressure of more than 50 kbars (Fabbro et al. 1990). The high pressure created during the melting and superheating of liquid at the end of laser pulse ejects the material within the focal volume at high speed.

Laser can also be utilized to cut the work piece of any material in desired geometrical shapes. It can even cut the work pieces which are normally difficult to cut by other machining processes. CO_2 laser and Nd:YAG laser are the most commonly used in cutting as these can deliver the required high powers for high speed cutting. UV lasers are mostly used for thin layer cuttings or organic material cutting. Plastics, polymers, composites, wood, rubber, papers, stones and crystals have been successfully machined by infrared lasers (Caiazzo et al. 2005; Lau et al. 1990). Some materials such as composites and gemstones can be readily cut with high quality using lasers, while they may be difficult to cut using other techniques. UV lasers can even cut polymers with negligible heat affected zone, because the photon energy is comparable to the bonding energy of the material dominated by photochemical process over photo-thermal (Znotins et al. 1987).

Drilling is one of the simplest and successful applications of industrial lasers. Drilling of holes in ceramic, silicon and polymer substrates is widely utilized in electronics industry. While, laser drilling of metals is used for fabrication of cooling channels in air turbine blades, tiny orifices for nozzles, etc. Holes less than 0.25 mm diameter can be drilled using laser with ease; especially for hard and brittle materials such as ceramics and gemstones (Forget et al. 1988). Large holes can be drilled by trepanning, i.e., by scanning the beam around the circumference of a circle.

Laser marking, scribing and texturing are important applications of laser micromachining besides cutting and drilling. In these applications, a very thin layer of material is ablated and a mark or pattern is formed (Qi et al. 2003). Permanent laser markings of almost all materials with high precision have considerable advantages over other techniques. It doesn't require any sample preparation or post treatment. Applications of laser markings range from shallow to deep-marking of hard and corrosion-resistant materials.

The general parameters which control laser machining are laser wavelength, beam shape, focal intensity of the laser on to the surface, pulse width, pulse repetition rate and working environment (vacuum/inert/air/liquid). Laser intensity is the main input process parameter that directly influences machining features such as material removal or HAZ. Generally, longer the wavelength, lower the absorption, hence decrease in material removal (Johan 2004). The output parameters are Material Removal Rate (MRR), machining geometry (kerf width, hole diameter, taper), surface quality (surface roughness, surface morphology), metallurgical characteristics (recast layer, heat affected zone, dross inclusion) and mechanical properties (hardness, strength).

1.1.1 Process Mechanism of Laser Induced Micromachining

When laser beam is focused on the target material, fraction of the energy is reflected and part of it is absorbed, the absorbed energy directly ablates the material by local heating in the focal region as depicted in Fig. 2.

The fraction of the incident power that is reflected from the surface depends on the polarization and angle of incidence of the laser as well as the reflectivity of the working medium (William and Mazumder 2010). Further, part of the incident power that is being absorbed by the work material propagates through the electron subsystem and then gets transferred to the lattice there by transferring to the ambient target material within the focal volume and its surrounding.

Based on the intensity of the laser, the surface undergoes melting, vaporization, plasma formation etc. At very high intensity, surface starts to vaporize before a significant melting depth of molten material is formed. The material gets removed through laser ablation. For laser pulse durations longer than microseconds, hydrodynamic ablation is the dominating phenomenon over the direct ablation. During laser cutting and drilling operations, there exists a time scale which allows the surface to heat to the vaporization temperature and remain there for some time. During the initial phase, the ablated particle surrounding the medium expands. This leads to the formation of recoil pressure which thereby helps in expulsion of the

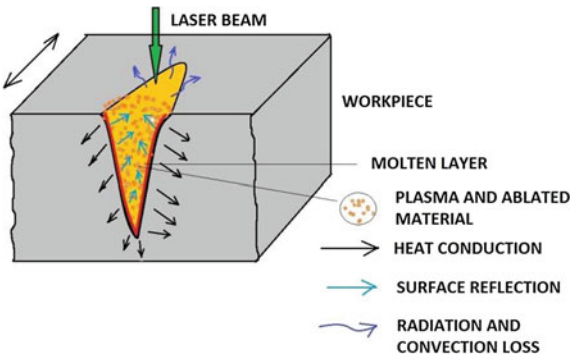

Fig. 2 Laser irradiation showing different phenomena involved

molten material from the irradiated region. In addition to this, there exist strong temperature gradients in the radial direction in the molten material due to the beam profile i.e. the center of the molten material is usually hotter than the outer. Thus, recoil pressure and temperature gradient drive the molten material out in the form of liquid droplets. The combination of vaporization and hydrodynamic ablation results into drilling or cutting the material in the focal region.

When the laser intensity is higher than that required to vaporize the work material, the vaporized material gets ionized. This leads to the formation of plasma at the vicinity of the work surface. With the formation of plasma, laser energy transmitted to the material depends on the density of the plasma. Below a certain critical value of the plasma density, laser energy is transmitted to the work material. When the critical value of the plasma density is reached, further transmission of laser energy onto the work material is cut off due to the absorption or reflection of the incident laser beam by laser induced plasma. Shock waves are generated when the above formed plasma expands, which is the basis for laser shock processing to improve residual stress of metal components (Sano et al. 1997). The sequence of processes in material removing via high power laser is depicted in Fig. 3.

Laser-induced micromachining can be performed under vacuum, in presence of low-high pressure gases and in liquid. The process of LIMM can be improved by placing the work piece in presence of magnetic field which controls the expansion of plasma. Figure 4a shows the schematic of LIMM under vacuum. Figure 4b that of in presence of liquid/air and Fig. 4c depicts the laser Induced Micromachining in presence of magnetic field. The process in LIMM can be improved using these careful choices of surrounding environment (Fabbro et al. 1990).

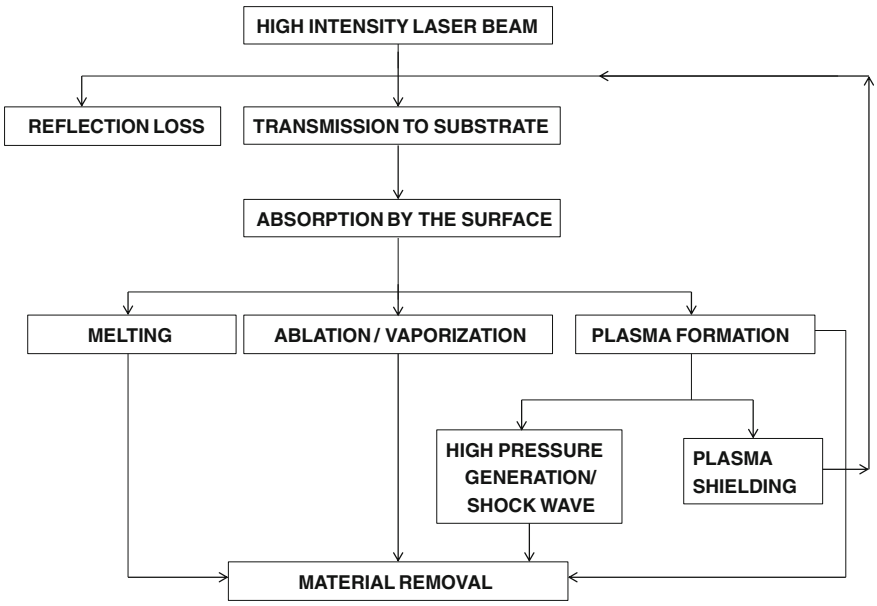

Fig. 3 Principle of LIMM

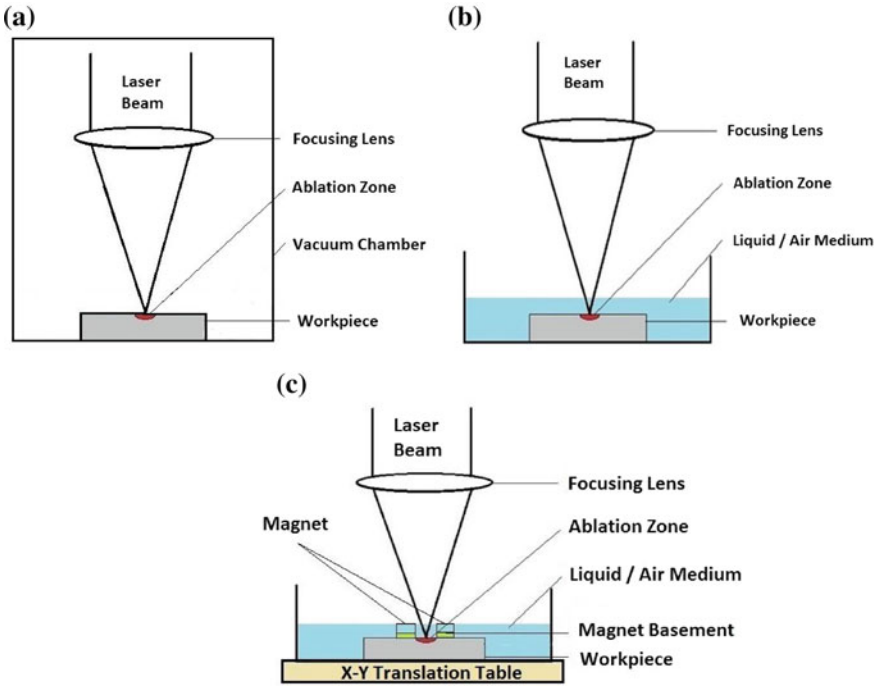

Fig. 4 **a** Laser induced micromachining in vacuum. **b** Laser induced micromachining in liquid/gas. **c** Laser induced micromachining process in magnetic field

1.2 Laser Induced Plasma Micromachining

Laser induced plasma (LIP) takes place when the energy of the incident laser exceeds the ablation threshold of the solid (Ali et al. 2014). Laser induced plasma micromachining (LIPMM) utilizes the ultra-short laser beam generated plasma in liquid medium to machine a component. The sequence of operations occurring in LIPMM is depicted in Fig. 5. It comprises of spot plasma based LIPMM process (S-LIPMM), Line-LIPMM process (L-LIPMM) and magnetically controlled LIPMM process (MC-LIPMM). In LIPMM, a high power laser is focused in a transparent liquid or air medium (shown in Fig. 5), there is a formation of laser induced plasma. The removal of material takes place when the generated plasma interacts with the substrate placed in the vicinity of LIP (Pallav et al. 2014). The duration of plasma, its size and density depend on the pulse duration, focal spot and the incident laser intensity.

Expansion of LIP replaces the medium and generates a large pressure on the workpiece surface. This exerted pressure by the plasma holds back the molten material. Eventually, plasma collapses after the termination of the laser beam, leading to the rushing of the surrounding medium back to fill the void. This results

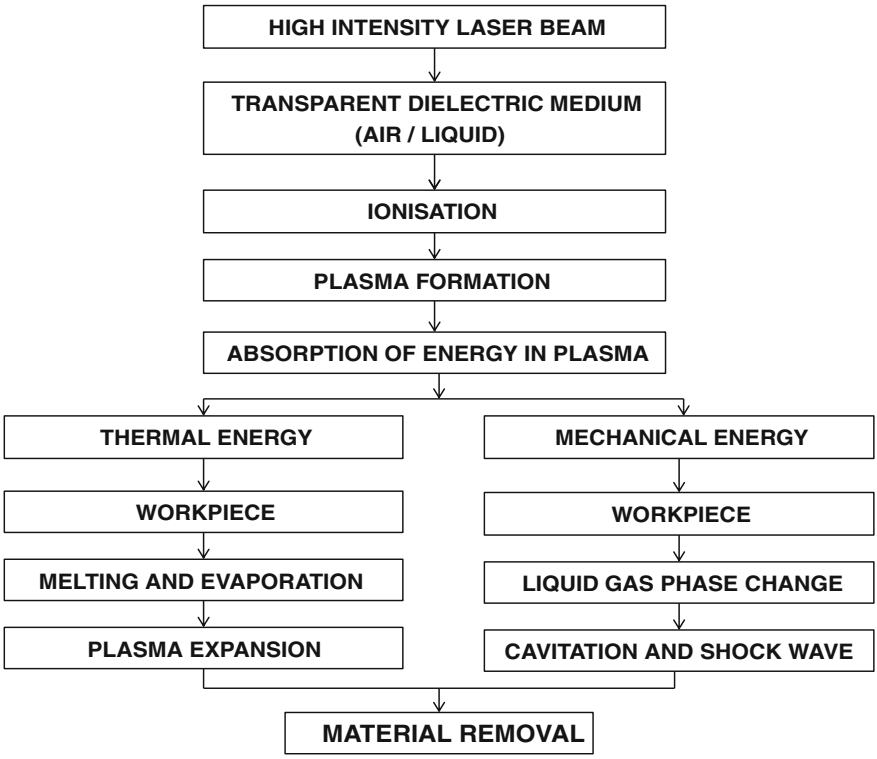

Fig. 5 Laser induced plasma micromachining

in an instantaneous expulsion of the material from the workpiece surface. Thus a crater is generated on the workpiece surface corresponding to every shot of LIP.

Micro-channel can be fabricated if the workpiece is moved with respect to the plasma in the focal region of the surface at a certain feed-rate in a preprogrammed motion. Overlapping of the craters in succession writes the micro channel (Pallav et al. 2014).

1.3 Laser Induced Plasma Assisted Ablation (LIPAA)

It utilizes the laser generated plasma as a by-product during laser ablation of a metallic target placed below a transparent workpiece (Hanada et al. 2006; Kadan et al. 2005; Zhang et al. 1999) as shown in the schematic of Fig. 6. In this process, laser beam is made to pass through a glass substrate which is transparent. Then the transmitted beam is focused on a solid target (typically a metal) placed behind the substrate so that the target is ablated resulting in plasma generation. The generated

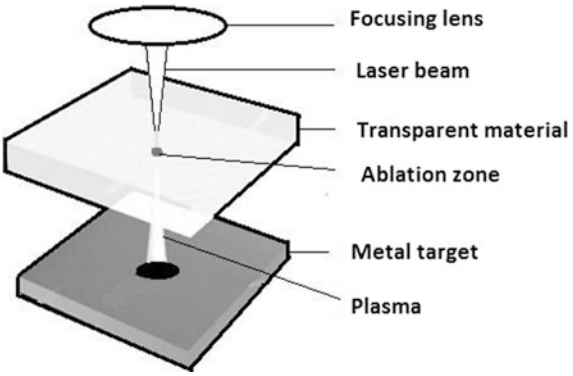

Fig. 6 Laser induced plasma assisted ablation

plasma is then used to machine the transparent material. This process has been widely applied for micromachining of various transparent hard and soft materials.

1.4 Advantages of LIMM

LIMM offers better machining efficiency and has various advantages over other micromachining processes. Some of the advantages are:

- Laser induced micromachining offers wide range of machining capabilities irrespective of the properties of the material.
- The issues of tool related problems such as tool wear, manufacturing of tool and cutting force are not required in laser induced micromachining.
- Greater process flexibility can be achieved by automation of laser system such as CNC incorporated laser system.
- The material removal rate is comparatively higher as compared to EDM, USM, EBM, etc.
- There is reduction in Heat Affected Zone (HAZ) due to very thin re-solidified layer.
- Machining can be performed with high precision in any geometry.

1.5 Limitations of LIMM

In spite of the various advantages of LIMM, it also has some unavoidable limitations.

- The machining depth is limited by the Rayleigh length.
- Heat affected Zone cannot be avoided completely in laser induced micromachining since the main material removal mechanism is thermal in nature.
- It is difficult to machine material possessing high reflectivity.

2 Literature Review on Laser Induced Micromachining

In view of the importance of laser induced micromachining (LIMM) in manufacturing of MEMS devices, micro-fluidic devices, relevant literatures on LIMM have been referred in this section. The following subsections deal with the papers related to modeling of temperature profile, HAZ and geometric features such as groove shape, width and depth of cut. Further, experimental findings towards the enhancement of laser induced micromachining are also discussed.

2.1 Numerical Studies of LIMM

Literature reports various numerical studies on LIMM mainly using finite element method (FEM) and finite difference method (FDM). Un-Chul and Francis (1972) developed a 1-D laser machining model that uses continuous, distributed and moving heat source for describing the temperature profile and thermal stress propagation for laser drilled holes in high purity fired-alumina ceramic substrate. Roy and Modest (1993) used moving CW gaussian beam profile to model evaporative laser machining of silicon nitride by incorporating temperature dependent properties such as specific heat and absorption coefficient using finite difference method. Pietro and Yao (1995) have developed a 3-D transient heat transfer model for the prediction of kerf geometry. Yu (1997) carried out a numerical study on the laser drilling and cutting process of copper plate using Ansys 5.0/ED which had incorporated with Ansys Parametric Design Language (APDL) to monitor and impose the changing boundary and loading conditions. The laser beam was modeled as a heat source moving on the workpiece in a prescribed manner.

Prusa et al. (1999) had developed a numerical model for the calculation of heat conduction losses, cutting speed and temperature distribution in HAZ in CO_2 laser cutting of thick materials. Meung and Jingwei (2001) introduced a finite element method for simulation of pulsed laser-cutting process in air to study amount of material removed and smoothness of groove shape with the gaussian pulsed laser beam, model in two dimensional unsteady heat conduction. Numerical simulation of LIMM was derived considering only the solid-liquid phase change using finite element method by Khalil and Sreenivasan (2005). Here, the enthalpy formulation was implemented in the Finite Element Method (FEM) based model.

Effect of multiple reflection, recoil pressure were incorporated in the numerical simulation of 1-D laser machining for alumina in addition to consideration of temperature dependent thermal conductivity and specific heat by using COMSOL multi-physics software (Samant and Dahotre 2009). Numerical simulation was also reported on laser machining of Carbon Fiber Reinforced Plastic composite material by Negarestani et al. (2009). A 3D finite element model was developed for predicting the transient temperature field, cut profile and heat affected zone. For the first time, the model employed the heterogeneous mesh for the composite with anisotropic material properties.

The thermal and optical properties of the target material change during the process of laser ablation. These temperature dependent material properties of the target material were taken into consideration for FEM model to predict the ablation depth and temperature distribution in pulsed laser ablation (Nikhil et al. 2010). The effect of plasma shielding on the incident laser flux was also considered in the model. Moscicki et al. (2011) developed a model which describes both the target heating, formation of the plasma and expansion. The model employed conservation of mass, momentum and energy which are solved by using Fluent™ software package.

Finite element modeling technique was employed to study the laser machining in air and water, in order to understand the underlying mechanism of underwater crack free machining. In this investigation, FEM based ANSYS™ software was employed to study the temperature distribution. The difference in heat convection coefficient was considered as the varying parameter in numerical simulation for laser machining in air and water (Yan et al. 2011).

2.2 Experimental Studies on LIMM

Investigations have been carried out on machining of glass matrix composite comprising SiC fibres in a borosilicate glass matrix. It has been reported that the material removal primarily depends on the pulse energy rather than the pulse duration (Ian et al. 1998). The effect of cutting parameters on the cut quality of ultra low carbon steel thin sheets has also been studied considering heat affected zone (HAZ) as the output parameter. It was found that HAZ increases with the increase in laser power and decreases with increase in scanning speed and gas pressure (Hanadi et al. 2008). Rajaram et al. (2003) reported that laser power plays a major role on the kerf width while feed rate played a minor role for experiments conducted on 4130 steel using CO_2 laser. Decreasing power and increasing feed rate generally led to a decrease in kerf width and HAZ. An increasing feed rate generally increases surface roughness and striation frequency. Comparison of CO_2 laser cutting with Continuous Wave (CW) and pulsed mode laser operation in presence of different gases namely argon, helium and nitrogen were carried out on titanium sheet (Rao et al. 2005). Use of helium as shear gas results in narrow HAZ and low dross as compared to that of Ar owing to high heat convection and shear stress provided by He gas. However, the laser cut edge produced in presence of He gas results in waviness of the cut. During the pulsed mode laser cutting of austenitic stainless steel sheet, rough surface and incomplete cutting has been observed on increasing the speed due to pulse separation and insufficient overlapping. While with continuous wave mode using Nd:YAG laser, increasing the speed with increase in power results in smoother surface, better quality and smaller kerf width (Ghany and Newishy 2005).

The cutting quality of laser machining depends on many input process parameters such as wavelength, pulse energy, pulse duration, optical and thermal properties of the material, composition, pressure of assist gas etc. Therefore,

optimization of these process parameters is required to obtain desired process performance. Sharma et al. (2010) employed Taguchi L_{27} orthogonal array to optimize the input parameters for both straight and curved cut profile using Nd: YAG laser for cutting of Nickel based super alloy thin sheet. It was observed that the optimum input parameter levels for curved cut profiles are entirely different from straight cut profiles except kerf width. Optimization of the multi performance for Nd:YAG laser cutting of nickel based superalloys has been carried out using grey relational analysis for quality characteristics of average kerf taper and average surface roughness (Sharma and Yadava 2011). It was observed that cutting speed was the most significant cutting parameter for minimizing the value of average kerf taper and average surface roughness. However the repetition rate, pulse width and back ground oxygen pressure were found to be less significant parameters.

The cross section of a drilled silicon nitride in air and water as reported by Noboru et al. (1988) using an Nd:YAG pulsed laser is shown in Fig. 7. In the air

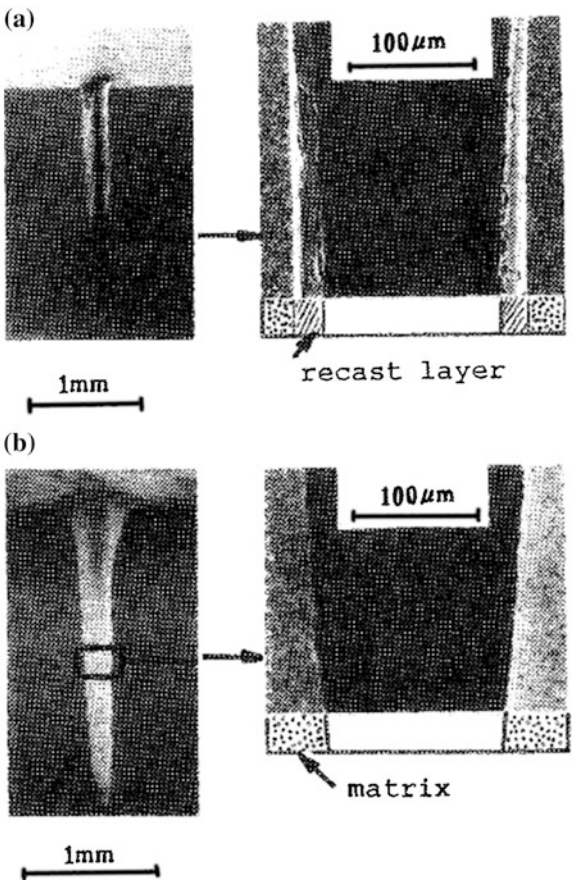

Fig. 7 Cross section of a silicon nitride ceramics drilled in **a** air **b** water with Q-switched power (pulse duration of 100 ns, laser energy of 5 mJ/pulse, Q-switching frequency of 1 kHz, processing time of 60 s, laser power density of 7.1×10^7 W/cm^2) (Noboru et al. (1988), with permission)

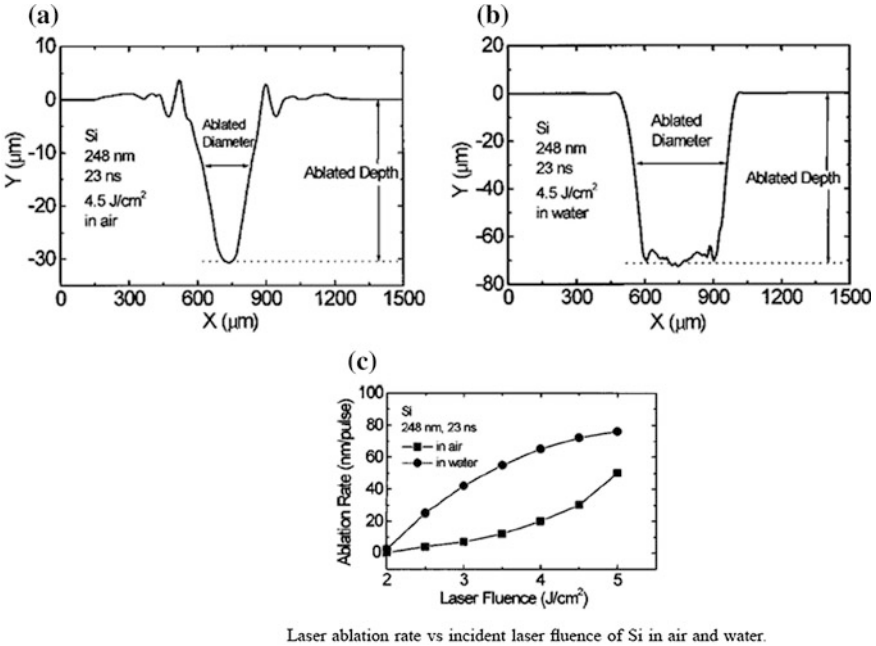

Fig. 8 **a** Profile of the ablated region of Si after 1000 pulse irradiation in air. **b** Profile of the ablated region of Si after 1000 pulse irradiation in water. **c** Laser ablation versus incident laser fluence of Si in air and water (Zhu et al. (2001), with permission)

ambient, a recast layer of about 20 μm thickness and micro-cracks were observed while these were absent in presence of water as back ground medium.

Ohara et al. (1997) did a study on infrared laser etching of micro coil pattern of Al bulk sample in water and air. The sample etched in air showed debris along the scanned line. The sample etched under water was devoid of any such debris. The sample etched in water showed deeper grooves compared to that of air. Probably the bubbles formed due to LIP in water helps in removing the debris.

Zhu et al. (2001) also reported that the laser ablation rate was enhanced in presence of water film above the workpiece. A KrF excimer laser with a wavelength of 248 nm and pulse duration around 23 ns was used for ablation of silicon sample. Figure 8 shows the profile of the ablated region in air and water. It shows that ablation rate in air in around 30 μm (Fig. 8a), whereas that of under water was 70 μm (Fig. 8b). It was also demonstrated that the ablation rate increases with the laser fluence for both the cases.

Kruusing et al. (1999) reported that machining in water of NdFeB magnet by short-pulsed laser provides clean grooves while machining in air results in grooves filled with molten material using Nd:YAG laser of 180 ns, 1.8 mJ, 1 kHz with varying feed rate.

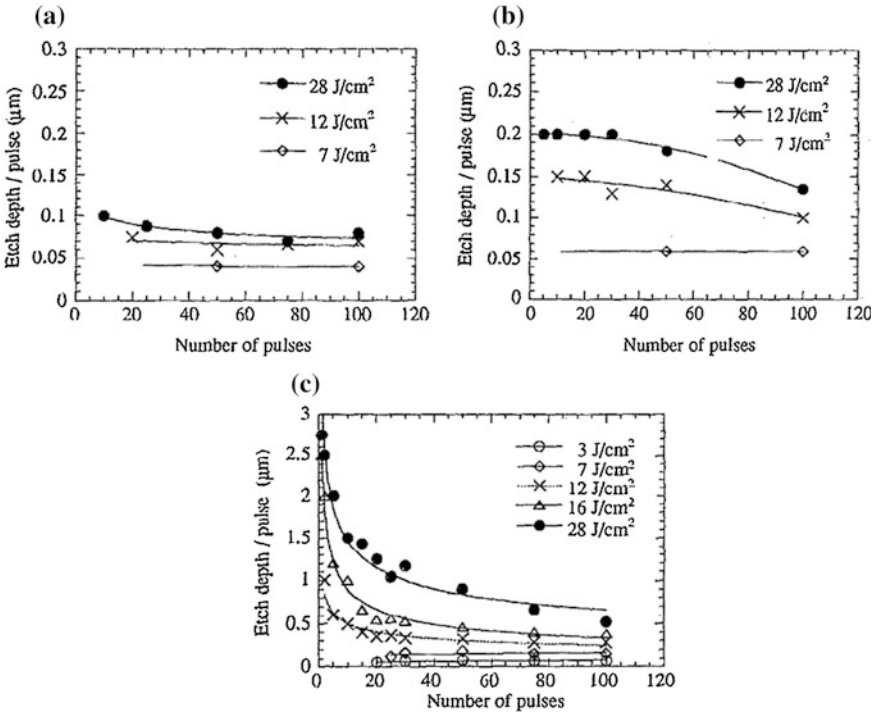

Fig. 9 **a** In the ambient atmosphere only. **b** With the addition of the argon gaseous cover. **c** With the addition of a water film on the treated surface (Dupont et al. (1995), with permission)

Dupont et al. (1995) carried out an experimental study on pulsed laser processing of stainless-steel alloy in ambient air, argon gas and also under a flowing water film on the material surface at atmospheric pressure. Figure 9 shows the variation of the etch depth per pulse as a function of number of pulses at the 532 nm laser wavelength. Figure 9a shows the effect of increase in number of pulses on the etch depth for different laser fluences, and that of in presence of argon in Fig. 9b. Figure 9c shows the effect in presence of water film on the treated surface. The etch depth was found to be maximum in presence of water film and decreases with the number of pulses at higher fluence.

Yuan-Jen et al. (2012) demonstrated the use of magnetic field in laser micromachining on highly reflective material Al6061 for drilling of micro hole. With the use of static magnetic field, the machining process could be enhanced by many folds in depth and the inlet diameter is reduced by 42 %. It was also observed that the roundness of the inlet was improved. The second harmonic of Nd:YAG laser at

532 nm wavelength, pulsed mode with maximum energy of 270 mJ, pulsed width of around 6 ns and frequency of 50 Hz were used in the experiments. The NdFeB permanent magnets with different arrangements were also tried in this work.

Zhang et al. (1999) performed micro-grating operation on workpieces of optically transparent materials: fused quartz and Pyrex glass using LIPAA. Kadan et al. (2005) also performed LIPAA for micro-marking and relieve grating in sapphire, silica and glass work material. Further, Hanada et al. (2006) demonstrated that crack free marking and color marking of glass material is possible using LIPAA.

Pallav and Ehmann (2010) introduced a new process, Laser Induced Plasma Micromachining (LIPMM) in which plasma generated in a transparent working medium is directly used to perform micromachining. Rajiv et al. (2013) extended this work, and observed that it can machine a wider variety of materials as compared to direct laser ablation. It was demonstrated that Line-LIPMM can be used for machining a line instead of a spot by optically manipulating the shape of the plasma. L-LIPMM can reduce the time for machining micro-textures over large areas by about six times, while retaining the multi-materials capability of Spot-LIPMM. Further, magnetic control-LIPMM (MC-LIPMM) was developed to manipulate the shape of the plasma. Additionally, MC-LIPMM can increase the length and reduce the width of the channel machinable with line plasma as well. Since no additional optics are required in MC-LIPMM the results showed that in-process manipulation of the shape and dimensions of the machined feature might be possible in MC-LIPMM, something which is not possible in laser ablation as the optics is required to be changed in the middle of a machining cycle.

Sarah and Ishan (2014) carried out an experimental study to show the feasibility of manipulating or controlling the plasma plume during laser machining using the magnetic field around the plasma plume in order to maximize the aspect ratio of the machined spot. Ultra short pulsed laser of Nd-YVO_4 solid state, 8 ps pulse duration at 532 nm wavelength and having Gaussian profile is used for the study. Polyamide (PA66) and aluminium alloy (A 5052) were used as substrates. Kerosene and distilled water was used as dielectric media.

Comparison of the different variation of LIPMM based on working parameters, dielectric and workpiece is tabulated in Table 1.

During laser ablation, formation of plasma occurs which comprises of electrons, ions and neutrals. This laser induced plasma absorbed the laser energy further. The energy is absorbed by means of photo-ionization and inverse Bremsstrahlung leading to increase in temperature and pressure. This can block laser radiation completely on the work piece (Moscicki et al. 2011). However, many researchers have been working on this aspect to machine different work materials including transparent and highly reflective materials by utilizing the generated plasma.

Table 1 Summary for variation of LIPMM

Sl. No.	Variation of LIPMM	Working parameters	Dielectric	Workpiece	Comparison	Remarks
1	S-LIPMM Rajiv et. al. (2013)	Nd-YVO_4 pulsed laser, 8 ps pulse duration, 0.12 W, 10 kHz	Distilled water	Semitransparent polycarbonate, opaque ABS polymer sheets, transparent alumina ceramic, polished silicon wafer, opaque sialon	Same condition followed for direct ablation	Transparent alumina could not be machined while sialon was machinable with depth of 6 µm in direct ablation while 18 µm was obtained using S-LIPMM
	L-LIPMM Rajiv et. al. (2013)		Kerosene, distilled water, EDM oil, mineral oil	AA5052	Same experimental conditions with varying dielectric	Kerosene—deposition on the sides and insides of the channel due to carbonization; Distilled water—no carbonization and comparable machined depth to kerosene EDM oil and mineral oil—no deposition, much lower machined depth; L-LIPMM has higher productivity than S-LIPMM and has 84% improved machining time
	MC-LIPMM Rajiv et. al. (2013)		Distilled water	AA5052	MC-LIPMM compared with S-LIPMM and L-LIPMM	MC-LIPMM results in longer channel with more uniform depth and width across the length of the channel; 200% increase in channel length

(continued)

Table 1 (continued)

Sl. No.	Variation of LIPMM	Working parameters	Dielectric	Workpiece	Comparison	Remarks
2	MC-LIPMM Sarah and Ishan (2014)	Nd-YVO_4 pulsed laser, 8 ps pulse duration, 0.13 W, 10 kHz	Kerosene, distilled water	PA 66; AA5052	Experiments conducted with varying magnetic configuration (8, 12, 1 neodymium magnet with 4400 Gauss surface field) and its location	Difference in aspect ratio observed; Only HAZ and no machining with LIPMM at same setting and focal point; Increase in aspect ratio upto 6 using external magnetic field
3	LIPMM Saxena et al. (2014)	Nd-YVO_4 pulsed laser, 8 ps pulse duration, 10–50 kHz, pulse energy 6 μJ	NaCl solution in distilled water, Fresh water	AA5052	Influence of the presence of salinity in dielectric	100% increase in depth at an optimum salinity of 2–4 g/100 ml

3 Preliminary Experimentation on Laser Induced Micromachining

In order to observe the effect of the sample scan speed on the surface roughness, laser micro channels were fabricated by focusing a second harmonic (532 nm) of a Q-switched Nd:YAG laser having pulse duration of a 10 ns, repetition rate of 10 Hz, focused to a size of 8.31×10^{-3} cm^2 on to a work sample in ambient environment. The work sample used for the experimentation is mild steel of dimension 30 × 10 × 3 mm. The sample is finely polished by mounting on a double disc rotating polishing machine. The polished work sample is then irradiated with second harmonic of a Q-switched Nd:YAG laser over a scanning length of 15 mm. The LIMM was performed at two different scan speeds. The experimental details are as listed in Table 2.

After irradiation with nanosecond laser in a single pass, formation of micro-channel has been observed. Figure 10 shows the pictorial view and profilometer image of the microchannel formed as observed by non-contact high precision

Table 2 Experimentation details

Experimental conditions		
Parameters	Sample 1	Sample 2
Energy per pulse	30 mJ	30 mJ
Focal length of the lens	150 mm	150 mm
Length of traverse	15 mm	15 mm
Speed	1800 step/s (540 µm/s)	900 step/s (270 µm/s)

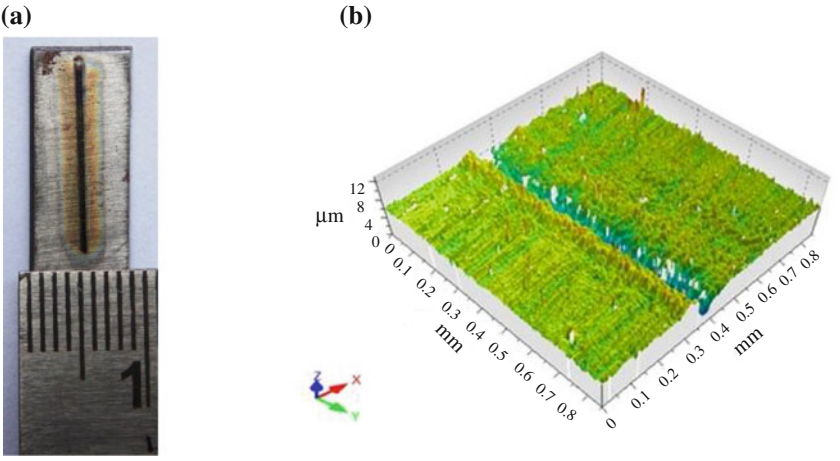

Fig. 10 **a** Pictorial view **b** Profilometer image of the microchannel for sample 1

profilometer for sample 1. It is observed from the figure that the formed channel is uniform throughout the traversed length. The width and the depth of the channel were being measured from the generated profilometer. For this, channel width and the depth of the cut were measured at four different sections along the channel length viz. section A-A, B-B, C-C and D-D as shown in Fig. 11. The sections were taken at equal intervals.

Figures 12 and 13 show the scan profile of the microchannel at scan speed of 540 and 270 μm/s respectively recorded by Profilometer.

The experimental results are listed in Table 3. The average value of the channel width was 114.7 and 146.5 μm for scan speed of 540 and 270 μm/s respectively. The average value of channel depth was 4.4 and 3.2 μm respectively. The decrease in the channel width with increase in scan speed is due to the reduction in

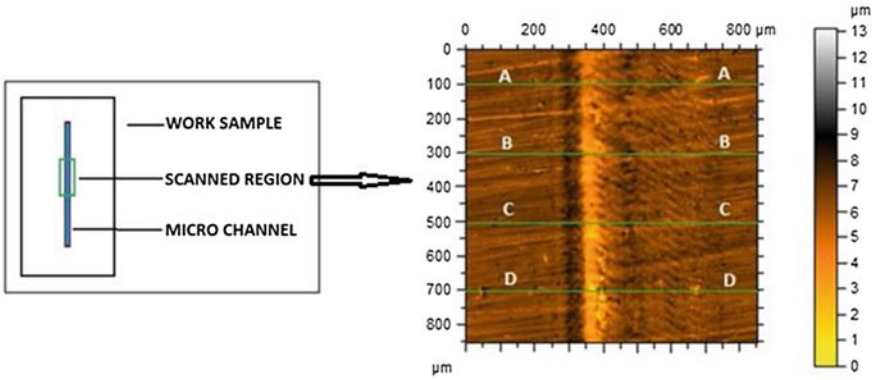

Fig. 11 Scanned area and roughness measured at different sections of the microchannel for sample1

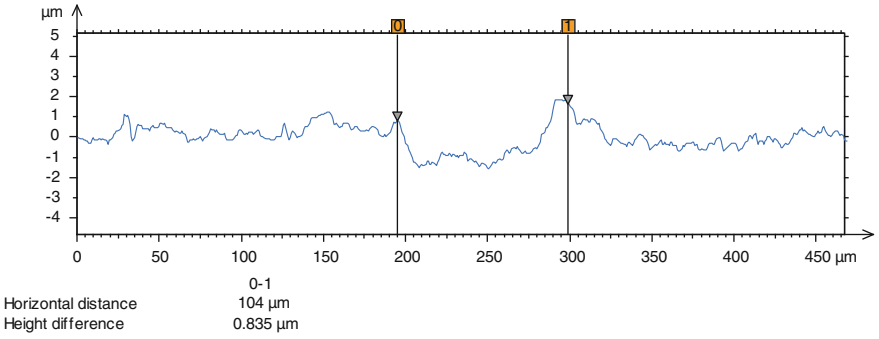

Fig. 12 Scan profile of the microchannel at scanning speed of 540 μm/s showing the width of the microchannel for sample 1

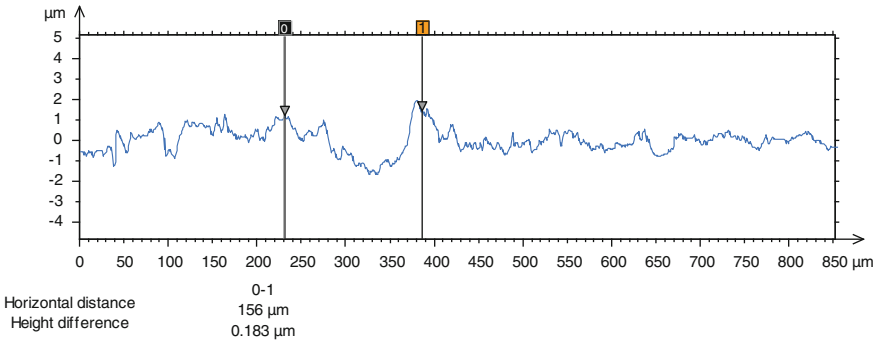

Fig. 13 Scan profile of the microchannel at scanning speed of 270 µm/s showing the width of the microchannel for sample 2

Table 3 Experimental results

Sample	Traverse speed (µm/s)	Section	Width (µm)	Depth (µm)
Sample 1	540	A-A	134	3.93
		B-B	121	4.6
		C-C	104	3.04
		D-D	100	5.94
Sample 2	270	A-A	141	3.51
		B-B	156	2.81
		C-C	121	4.01
		D-D	168	2.46

interaction time of the laser beam with the work sample at a given location. The decrease in the depth at lower scan speed could be due to the formation of recast layer in the channel.

4 Summary

After an in-depth study of the available literature related to LIMM, it has been observed that many attempts have been made in modeling of LIMM towards complete phenomenon. Initially, modeling of LIMM has been developed considering only the direct vaporization of the substrates. Later, modeling of the phenomenon considering multiphase viz. liquid, gas and plasma has also been carried out. Simultaneously, various time dependent physical properties of the material and the process are being incorporated in the trend. Above all of these, it is found that a very scant amount of work has been done on modeling of LIMM in liquid medium and in presence of magnetic field and electric field. Therefore, this area of research

is still open for further advancement and to improve the understanding of the process and modeling so as to match the experimental observations and improve the precision.

The quality of laser machined component depends on many input process parameters viz; wavelength, repetition rate, pulse energy, pulse duration, optical and thermal properties of the material, composition and pressure of assist gas etc. Therefore, optimization of these process parameters is required to obtain the desired performance. Varying the machining medium has a major impact on the quality of the machined component. Various theories have been reported to study this effect. The performance of LIMM can further be enhanced with the application of the magnetic field.

References

Ali, A. K. H., Kadhim, A. A., & Mohammed, R. A. (2014). Investigation of some physical parameters of laser induced copper plasma. *Asian Journal of Applied Sciences, 2*, 151–157.

Caiazzo, F., Curcio, F., Daurelio, G., & Minutolo, F. M. C. (2005). Laser cutting of different polymeric plastics (PE, PP and PC) by a CO_2 laser beam. *Journal of Materials Processing Technology, 159*, 279–285.

Di Pietro, P., & Yao, Y. L. (1995). A numerical investigation into cutting front mobility in CO_2 laser cutting. *International Journal of Machine Tools and Manufacture, 35*(5), 673–688.

Dupont, A., Caminat, P., & Bournot, P. (1995). Enhancement of material ablation using 248, 308, 532, 1064 nm laser pulse with a water film on the treated surface. *Journal of Applied Physics, 78*(3), 2022–2028.

Fabbro, R., Fournier, J., Ballard, P., Devaux, D., & Virmont, J. (1990). Physical study of laser-produced plasma in confined geometry. *Journal of Applied Physics, 68*, 775–784.

Forget, P., Jeandin, M., Lechervy, P., & Varela, D. (1988). Laser drilling of a superalloy coated with ceramic. *The metallurgical society* (pp. 553–562).

Ghany, K. A., & Newishy, M. (2005). Cutting of 1.2 mm thick austenitic stainless steel sheet using pulsed and CW Nd:YAG laser. *Journal of Materials Processing Technology, 168*, 438–447.

Hanada, Y., Sugioka, K., & Midorikawa, K. (2006). Laser-induced plasma-assisted ablation (LIPAA): Fundamental and industrial applications (Vol. 6261, pp. 626111-1-15). In: *Proceedings of SPIE*

Hanadi, G. S., Mohy, S. M., Yehya, B., & Wafaa, A. A. (2008). CW Nd:YAG laser cutting of ultra low carbon steel thin sheets using O_2 assist gas. *Journal of Materials Processing Technology, 196*, 64–72.

Ian, P. T., Tony, P. H., & Ian, P. R. (1998). Nd-YAG laser machining of SiC fibre/borosilicate glass composites. Part I. Optimisation of laser pulse parameters. *Composites Part A, 29A*, 947–954.

Johan, M. (2004). Laser beam machining (LBM), state of the art and new opportunities. *Journal of Materials Processing Technology, 149*, 2–17.

Kadan, V. M., Blonsky, I. V., Salnikov, V. O., & Orieshko, E. V. (2005). Effect of laser induced plasma in machining of transparent materials. *Proceedings of SPIE 5715, Micromachining and Microfabrication Process Technology X*, *130*, 130–137.

Khalil, A. A. I., & Sreenivasan, N. (2005). Study of experimental and numerical simulation of laser ablation in stainless steel. *Laser Physics Letters, 2*, 445–451.

Kruusing, A., Uusimaki, A., Petretis, Br, & Makarova, O. (1999). Micromachining of magnetic materials'. *Sensors and Actuators A, 74*(1–3), 45–51.

Lau, W. S., Lee, W. B., & Pang, S. Q. (1990). Pulsed Nd: YAG laser cutting of carbon fibre composite materials. *CIRP Annals—Manufacturing Technology*, *39*, 179–182.

Meung, J. K., & Jingwei, Z. (2001). Finite element analysis of evaporative cutting with a moving high energy pulsed laser. *Applied Mathematical Modelling, 25*, 203–220.

Moscicki, T., Hoffman, J., & Szymanski, Z. (2011). Modelling of plasma formation during nanosecond laser ablation. *19th Polish National Fluid Dynamics Conference (KKMP), Poznan, 63*, 99–116.

Negarestani, R., Sundar, M., Sheikh, M. A., Mativenga, P., Li, L., Li, Z. L., et al. (2009). Numerical simulation of laser machining of carbon-fibre-reinforced composites. *Proceedings of IMechE, 224*, 1017–1662.

Nikhil, A. V., Upendra, V. B., & Suhas, S. J. (2010). A finite element model to predict the ablation depth in pulsed laser ablation. *Thin Solid Films, 5*(19), 1421–1430.

Noboru, M., Shuichi, I., Yasutomo, F., & Ken, I. (1988). Pulsed laser processing of ceramics in water. *Applied Physics Letters, 52*, 1965–1966.

Ohara, J., Nagakubo, M., Kawahara, N., & Hattori, T. (1997). High aspect ratio etching by infrared laser induced micro bubbles. In: *Proceedings of the IEEE Tenth Annual International Workshop on Micro Electro Mechanical System* (pp. 175–179), New York: IEEE.

Pallav, K., & Ehmann, K. F. (2010). Feasibility of laser induced plasma micromachining (LIP-MM). *Precision Assembly Technologies and Systems*, *315*, 73–80

Pallav, K., Han, P., Ramkumar, J., Nagahanumaiah, & Ehmann, K. F. (2014), Comparative assessment of the laser induced plasma micromachining and the micro-EDM processes. *Journal of Manufacturing Science and Engineering*, *136*, 011001-1-16.

Prusa, J. M., Venkitachalam, G., & Molian, P. A. (1999). Estimation of heat conduction losses in laser cutting. *International Journal of Machine Tools and Manufacture, 39*, 431–458.

Qi, J., Wang, K. L., & Zhu, Y. M. (2003). A study on the laser marking process of stainless steel. *Journal of Materials Processing Technology, 139*, 273–276.

Rajaram, N., Sheikh-Ahmad, J., & Cheraghi, S. H. (2003). CO_2 laser cut quality of 4130 steel. *International Journal of Machine Tools and Manufacture, 43*, 351–358.

Rajiv, M., Ishan, S., Kornel, E., & Jian, C. (2013). Laser-induced plasma micromachining (LIPMM) for enhanced productivity and flexibility in laser based micromachining processes. *CIRP Annals—Manufacturing Technology*, *6*, 211–214.

Rao, B. T., Kaul, R., Tiwari, P., & Nath, A. K. (2005). Inert gas cutting of titanium sheet with pulsed mode CO_2 laser. *Optics and Lasers in Engineering, 43*, 1330–1348.

Roy, S., & Modest, M. F. (1993). CW laser machining of hard ceramics-I. Effects of three-dimensional conduction, variable properties and various laser parameters. *International Journal of Heat and Mass Transfer, 36*, 3515–3528.

Samant, A. N., & Dahotre, N. B. (2009). Laser machining of structural ceramics—A review. *Journal of the European Ceramic Society, 29*, 969–993.

Sano, Y., Mukai, N., Okazaki, K., & Obata, M. (1997). Residual stress improvement in metal surface by underwater laser irradiation. *Nuclear Instruments and Methods in Physics Research B, 121*, 432–436.

Sarah, W., & Ishan, S. (2014). A preliminary study on the effect of external magnetic fields on laser-induced plasma micromachining (LIPMM). *Manufacturing Letters*. doi:http://dx.doi.org/10.1016/j.mfglet.2014.02.003.

Saxena, I., Ehmann, K., & Cao, J. (2014). Productivity enhancement in laser induced plasma micromachining by altering the salinity of the dielectric media. *ICOMM—2014*, (Vol. 93).

Sharma, A., & Yadava, V. (2011). Optimization of cut quality characteristics during Nd:YAG laser straight cutiing of Ni-based superalloy thin sheet using grey relational analysis with entropy measurement. *Materials and Manufacturing Processes, 26*, 1522–1529.

Sharma, A., Yadava, V., & Rao, R. (2010). Optimization of kerf quality characteristics during Nd: YAG laser cutting of nickel based superalloy sheet for straight and curved cut profiles. *Optics and Lasers in Engineering, 48*, 915–925.

Silfvast, W. T. (2004). *Laser fundamentals* (2nd ed.). Cambridge: Cambridge University Press.

Un-Chul, P., & Francis, P. G. (1972). Thermal analysis of laser drilling processes. *IEEE Journal of Quantum Electronics, 8*, 112–119.

William, M. S., & Mazumder, J. (2010). *Laser material processing* (4th ed.). Berlin: Springer.

Yan, Y., Li, L., Sezer, K., Wang, W., Whitehead, D., Ji, L., et al. (2011). CO_2 laser underwater machining of deep cavities in alumina. *Journal of the European Ceramic Society, 31*, 2793–2807.

Yu, L. M. (1997). Three-dimensional finite element modelling of laser cutting. *Journal of Materials Processing Technology, 63*, 637–639.

Yuan-Jen, C., Chia-Lung, K., & Nai-Yu, W. (2012). Magnetic assisted laser micromachining for highly reflective metals. *Journal of Laser Micro/nanoengineering, 7*, 254–259.

Zhang, J., Sugioka, K., & Midorikawa, K. (1999). Micromachining of glass materials by laser-induced plasma assisted ablation (LIPAA) using a conventional nanosecond laser. *Proceedings SPIE conference on Laser Applications in Microelectronics and Optoelectronic Manufacturing IV, 3618*, 363–369.

Zhu, S., Lu, Y. F., Hong, M. H., & Chen, X. Y. (2001). Laser ablation of solid substrates in water and in ambient air. *Journal of Applied Physics, 89*(4), 2400–2403.

Znotins, T. A., Poulin, D., & Reird, J. (1987). Excimer lasers: An emerging technology in materials processing. *Laser Focus, 23*, 54–70.